Thin Solid Films 534 (2013) 497–502

Contents lists available at SciVerse ScienceDirect

Thin Solid Films

journal homepage: www.elsevier.com/locate/tsf

A theoretical approach to photosynthetically active radiation silicon sensor

M.J.L. Tamasi, M.G. Martínez Bogado *

Consejo Nacional de Investigaciones Científicas y Técnicas, CONICET, Departamento de Energía Solar-Gerencia de Investigación y Aplicaciones, Centro Atómico Constituyentes, Comisión Nacional de Energía Atómica (CNEA), Av. General Paz 1499, (1650) San Martín, Buenos Aires, Argentina

ARTICLE INFO

Article history:
Received 17 October 2011
Received in revised form 18 February 2013
Accepted 20 February 2013
Available online 5 March 2013

Keywords:
Photosynthetically active radiation
Radiometers
Sun sensors
Silicon devices

ABSTRACT

This paper presents a theoretical approach for the development of low cost radiometers to measure photosynthetically active radiation (PAR). Two alternatives are considered: a) glass optical filters attached to a silicon sensor, and b) dielectric coating on a silicon sensor. The devices proposed are based on radiometers previously developed by the Argentine National Atomic Energy Commission. The objective of this work is to adapt these low cost radiometers to construct reliable instruments for measuring PAR.

The transmittance of optical filters and sensor response have been analyzed for different dielectric materials, number of layers deposited, and incidence angles. Uncertainties in thickness of layer deposition were evaluated.

1. Introduction

Silicon photovoltaic solar sensors are generally used to measure radiation in the 300 to 1100 nm wavelength band where they produce a current closely proportional to the intensity of the incident radiation. These devices have both terrestrial and space applications. In terrestrial uses, solar radiometers are frequently employed to measure solar radiation due to their low cost in comparison with pyranometer thermoelectric sensors, whose operation is based on thermopiles. In space applications, spacecrafts include such devices for attitude determination and control. These types of sensors are known as primary sensors, or coarse solar sensors, and are used, for instance, to orient the solar panels [1]. The small mass and large field of view, are their main advantages. Because of this, coarse solar sensors are widely used in space missions [2–4].

The semiconductor photovoltaic radiometers use a photodiode or a silicon cell as the sensitive element. The radiant flux incident on its surface generates a current which is mainly proportional to the irradiance, but the response of these devices depends on the radiation spectrum, so their application is limited. A radiometer can be calibrated using a reference thermoelectric pyranometer whose spectral response is flat. However, its low cost (a factor of ten or lower), high power output, and its almost instantaneous response, make the photovoltaic radiometers particularly useful in low cost networks, for use as secondary instruments to interpolate thermal pyranometer systems (or stations), and for detection of fast and/or small fluctuations of irradiance.

The radiometer manufacturing technology is well known. However, the advantages of developing these devices locally lie in the possibility of providing university and science and technology agencies a reliable tool, at lower cost and faster availability than commercial instruments of foreign origin.

Although measured or interpolated data of global solar irradiation are available, published values of photosynthetically active radiation (PAR) are scarce. PAR intensity, with wavelength range between 400 and 700 nm [5] is a necessary input in applications dealing with plant physiology, biomass production and natural illumination in greenhouses. Some local measurements performed in Argentina can be found in references [6] and [7].

The determination of these variables is to:

- assess relevant agricultural data, such as influence of solar radiation at ground level on the yield of crops or on growth of a particular crop,
- evaluate evapotranspiration rate of a community or ecosystem and,
- study the dynamics of water cycles and, consequently, its evolution status in the context of the global climate change.

2. PAR and radiometers

Incident PAR is required to model photosynthesis of single plant leaves or complex plant communities. It is an important parameter in comprehensive studies of radiation climate, remote sensing of vegetation, radiation regimes of plant canopy, and also in the development of models of photosynthesis and vegetation productivity [8]. In this spectral range, an important absorption of light by vegetal chlorophyll is produced, causing in certain sub-regions significant morphogenetic and ontogenetic effects [9]. The accurate determination and clear understanding of the PAR component are required in many applications

* Corresponding author. Tel.: +54 11 6772 7837; fax: +54 11 6772 7121.
E-mail address: mbogado@tandar.cnea.gov.ar (M.G. Martínez Bogado).
URL: http://www.tandar.cnea.gov.ar (M.G. Martínez Bogado).

0040-6090/$ – see front matter © 2013 Elsevier B.V. All rights reserved.
http://dx.doi.org/10.1016/j.tsf.2013.02.061

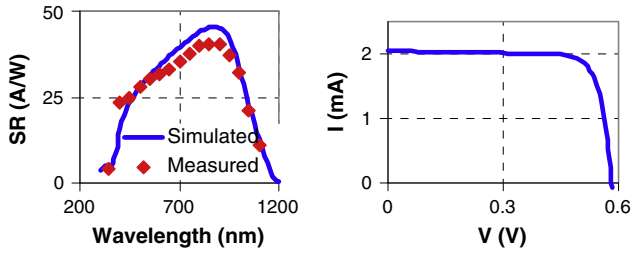

Fig. 1. Typical measured and simulated spectral response and I–V curve obtained using PC-1D4 code.

such as net primary productivity and carbon cycle modeling [10,11]. In general, direct measurement data of the PAR component are not available and in many instances the use of either modeling simulations or techniques relying upon empirically derived estimates has filled this gap [12,13].

The Solar Energy Department (DES) of the Argentine National Atomic Energy Commission (CNEA) performs R&D activities related with photovoltaic solar energy conversion for space and terrestrial applications. The development of low cost photovoltaic radiometers began by 1998, to measure global solar radiation and more recently to build PAR radiometers [14]. This project was developed through a cooperation between DES-CNEA and the Study Group of Solar Radiation at the National University of Luján (GERSolar-UNLu).

First prototypes of PAR radiometers were developed using a commercial filter and were calibrated by GERSolar. In reference [14], the behavior of one of these radiometers is compared with a commercial unit. The manufacturing technology of solar sensors is similar to that employed for silicon solar cells. Based on previous experience [1], the sensors can be designed to fulfill requirements for either space or terrestrial applications.

This paper proposes a different configuration to adapt sensor spectral response to build PAR radiometers using well known techniques for deposition of dielectric materials. To achieve this, we present a theoretical study of the development of filters employing dielectric layers.

3. Sensor characteristics

Rectangular solar cells with a circular active area (about 0.8 mm^2) and a n^+pp^+ structure have been fabricated on commercial Czochralski monocrystalline Si wafers, boron-doped, with resistivity of about 2 Ω cm. A simple one-step diffusion process at 870 °C [15] has been used for generating the n^+pp^+ structure (P dopant from a $POCl_3$ liquid source n^+ region, and evaporated Al for p^+ region). Sheet resistance of the n^+ region was 60–90 Ω/sq. The active area of these sensors is defined by photolithography. Standard Ti–Pd–Ag multilayers were evaporated to produce front and rear contacts.

I–V curves were obtained using a solar simulator Class C AM1.5, adjusted to deliver a radiation intensity equivalent to 1 kW/m^2, measured with a reference cell. Short circuit current (I_{sc}), open circuit voltage (V_{oc}), maximum power, fill factor and other parameters were thus obtained.

Table 1
Optical index and quarter-wavelength optical thickness for different dielectric materials.

Material	n (@ 550 nm)	Thickness (Å)
MgF_2	1.35	797
Na_3AlF_6	1.38	815
Al_2O_3	1.78	618
ZnS	2.3	957
TiO_2	2.74	803
Ta_2O_5	2.09	1053

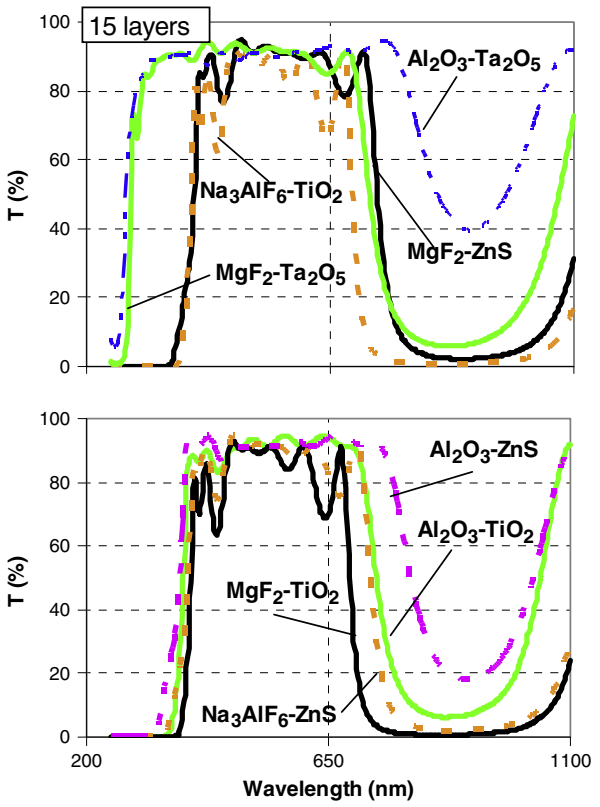

Fig. 2. Transmission spectra calculated for 15 layers of eight different combinations of materials.

Spectral response (SR) measurements have been performed in accordance to ASTM E 1021-84 [16], using equipment designed and manufactured by DES. Fig. 1 shows typical simulated and measured sensor SR curves. Both SR and I–V curves (Fig. 1) were simulated using the PC1D code [17]. This tool allows obtaining SR curves, characteristic electrical parameters, and carrier density, and to analyze modification of device characteristics as functions of surface reflectance, minority carrier lifetime, junction depth, and doping. Up to 3 dielectric coatings can be simulated and it is possible to shape the illuminating spectrum and make use of other tools for device design.

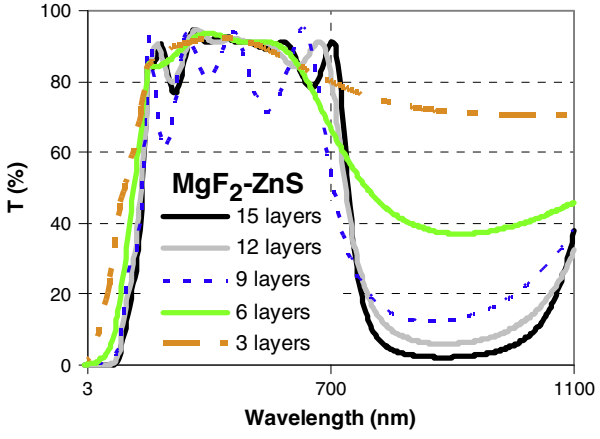

Fig. 3. Transmittance as a function of number of layers of MgF_2–ZnS.

Table 2
I_{sc} calculated for a sensor with filters of 12 and 15 layers of MgF_2–ZnS deposited on glass.

Configuration	I_{sc} (mA)
No filter	2.07
With ideal filter	0.99
12 layers	1.09
15 layers	1.05

The PC-1D4 is a simulation program for quasi-one-dimensional semiconductor devices that solves numerically the nonlinear coupled equations of electron and hole transport. To simulate electrical and electronic characteristics (voltage–current curve and spectral response curves respectively) of the manufactured devices, the following input parameters for solar cells with structure of Si n^+pp^+ were used:

- Device area: 0.8 mm^2
- Thickness: 300 μm
- Material: Si
- P-type background doping: 1.5×10^{16} cm^{-3}
- Front diffusion: N-type, 3.3×10^{19} cm^{-3}
- Rear diffusion: P-type, 2×10^{18} cm^{-3}
- Bulk recombination: $\tau_n = \tau_p = 20$ μs
- Front and rear surface recombination: $S_n = S_p = 1.9 \times 10^6$ cm/s
- Front reflectance from empirical measurement 40 nm SiO_2.

The parameters that were measured experimentally were: device area, sample thickness and base and emitter doping and minority carrier effective lifetime. The curves simulated with PC-1D4 are in good agreement with measurements performed on fabricated devices.

4. Design of an on-glass optical filter

4.1. Number of layers and materials

Band-pass multilayer transmitting interference filters were evaluated. Many filter types can be realized using only two different coating materials, one with high index of refraction and one with a low index. In the mid-infrared region (1800–8000 nm) the best choice available is: Ge (high-index) and Si (low-index). In the visible and near infrared region (400–1800 nm) ZnS and TiO_2 are commonly used as high index materials and MgF_2 and silicon oxide as low-index materials.

As a first step we designed an on-glass broadband pass optical filter to allow transmission in PAR band by simulating deposition of multilayer dielectric materials (of high and low index) [18]. The stack on glass has the form:

$$1.6(L/2\ H\ L/2)^m \quad (1)$$

where H is a quarter-wavelength optical thickness for the high index material (n = 2.4 for TiO_2, n = 2.3 for ZnS @ 550 nm), L is a quarter-wavelength optical thickness for the low index material (n = 1.38 for MgF_2, n = 1.35 for Na_3AlF_6 @ 550 nm), and m is the number of sets of three layers each to be deposited. The substrate adopted was glass with n = 1.52 at 550 nm.

This configuration was chosen for simplicity. Other filters combine designs of low-pass and high-pass filters, and two low-pass filters but they all require the superposition of at least 30 layers [18].

In this study we have used the GPL Optical (0.1.8 version) [19] simulation program for multilayer systems developed by Bologna University. By using a generalized scattering matrix method this program can treat multilayers with any number of coherent and incoherent layers, stacked in any order, and for any incidence angle. This code can estimate total light reflectance (R), transmittance (T), internal absorption and internal energy flux as a function of wavelength. The input parameters of the program are: refractive indices (n, k) for different materials:

Table 3
Calculation of I_{sc} with 15 layers of MgF_2–ZnS filter, an ideal filter and differences between them as a function of angles of incidence.

Angle α	I_{sc} sim. (mA) (15 layers)	I_{sc} (mA) × cos α (ideal filter)	Difference (mA)
0°	1.05	0.99	0.06
20°	1.01	0.93	0.08
40°	0.94	0.76	0.18
45°	0.93	0.70	0.23
60°	0.90	0.50	0.40
80°	0.61	0.17	0.44

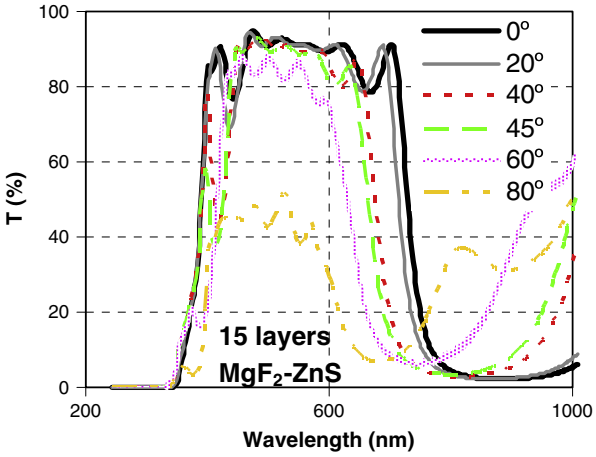

Fig. 4. Transmittance for different angles of incidence.

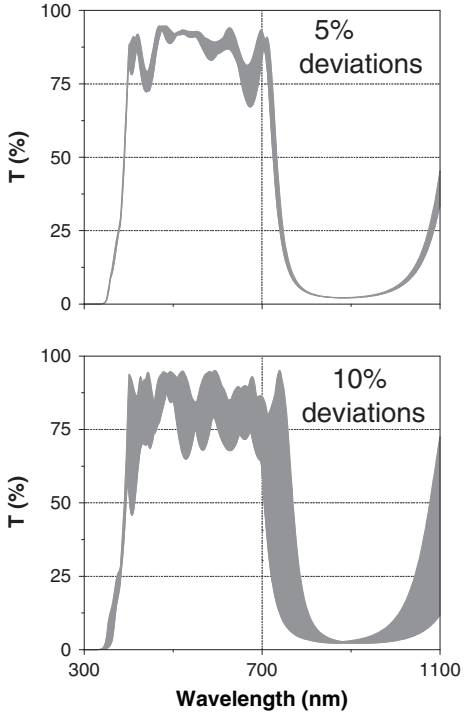

Fig. 5. Calculated transmittance spectra of 15-layer MgF_2–ZnS coating considering random fluctuations with standard deviations of 5 and 10%.

Table 4
Calculation of I_{sc} with estimated error on glass filter with 15 layers of MgF_2–ZnS.

Sensor configuration	I_{sc} (mA)
No filter	2.07
With ideal filter	0.99
15 layer filter	1.05
15 layer filter and 5% standard deviation	1.04
15 layer filter and 10% standard deviation	1.10

substrates (glass or Si) and dielectric layers (ZnS and MgF_2), thicknesses and angles of incidence.

Various combinations of high and low index dielectric materials were considered, as well as the transmittance for several sets of 15 layers. Materials used are shown in Table 1, which includes thicknesses and optical indices. The design wavelength was set to 550 nm (center of the range considered).

Eight different combinations of materials were analyzed. Transmittance is shown in Fig. 2. As can be seen each structure presents advantages and disadvantages. Some of them, such as those containing Ta_2O_5, have a relatively flat response but deviate from the range of wavelengths of interest because transmission starts before 300 nm and extends beyond the desired cutoff at 700 nm. In other combinations, such as cryolite and MgF_2 with TiO_2, they present many oscillations in the transmission region.

The combination of MgF_2 and ZnS was selected because it features a transmittance curve according to requirements, and furthermore, these materials are widely used for optical coatings. To determine the minimum number of layers required, filters with 3, 6, 9, 12 and 15 layers were simulated. Fig. 3 shows changes in transmittance when adding sets of 3-layers. After depositing 9 layers the filter starts to behave as expected.

The I_{sc} of a typical sensor with filters of 12 and 15 layers was calculated to evaluate current as a function of the number of layers. This parameter was done from a standard spectrum, using filter transmittance and the known spectral response of the sensor. 9-layer filters were not considered due to the oscillations produced in the bandpass, and a poorly defined cutoff for longer wavelengths. Additionally, a comparison was done against an "ideal filter" defined as having 100% transmittance between 400 and 700 nm and 0% in the rest of the spectrum. The results are shown in Table 2. Difference between I_{sc} calculated for 12 and 15-layer filters and that of the ideal filter was 10% and 6%, respectively.

Table 5
I_{sc} calculation for different number of MgF_2–Zn layers on Si sensor.

Sensor configuration	I_{sc} (mA)
No filter	2.07
With ideal filter	0.99
15 AR layers	1.10
12 AR layers	1.13
9 AR layers	1.20

Table 6
Calculation of I_{sc} for different dielectric coatings on Si sensor.

Dielectric coating	I_{sc} (mA)
Ideal filter	0.99
MgF_2–ZnS	1.10
Ta_2O_5–Mg_2F	1.22
Al_2O_3–TiO_2	1.39
Al_2O_3–ZnS	1.69

4.2. Variation of the transmittance as a function of the angle of incidence

These radiometers are generally installed outdoors, or in greenhouses, to obtain measurements during several months. Daily values are normally collected. Although the sun is changing position along the day, this type of low cost instrument is installed in horizontal position, without any sun-tracking hardware. Since transmittance of optical filters varies with the angle of incidence we evaluated a 15-layer filter working at different angles of incidence to estimate uncertainties in PAR measurement throughout a day. These results are shown in Fig. 4.

Table 3 shows calculated values of transmittance for 15-layer filter at several incidence angles. Due to changes in transmittance the difference in the value of I_{sc} calculated at angles of 45°, or larger, with respect to normal incidence, is higher than 10%. Values obtained are compared with I_{sc} cos α for an ideal filter. It can be observed that differences increase for increasing angles.

4.3. Evaluation of uncertainties in layer thicknesses

To estimate the precision required in layer deposition, random fluctuations in layer thicknesses were introduced in theoretical simulations. These fluctuations were simulated following normal distributions with 5 and 10% standard deviations (Fig. 5).

Differences in absolute values between the simulated curve areas, with and without random fluctuations in thicknesses, were calculated.

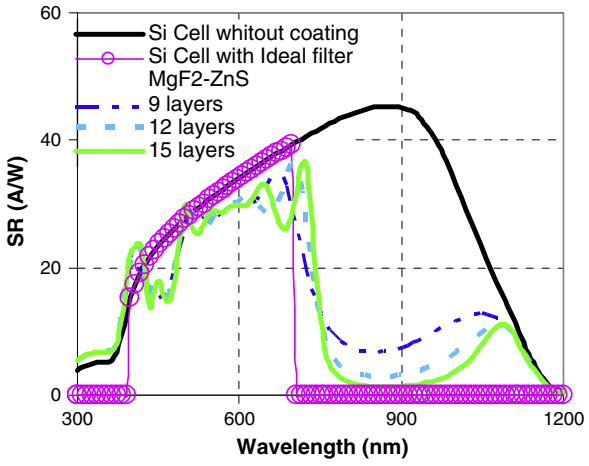

Fig. 6. Simulated spectral response of a sensor without coating, with 9, 12 and 15 layers of MgF_2–ZnS, and with an ideal filter.

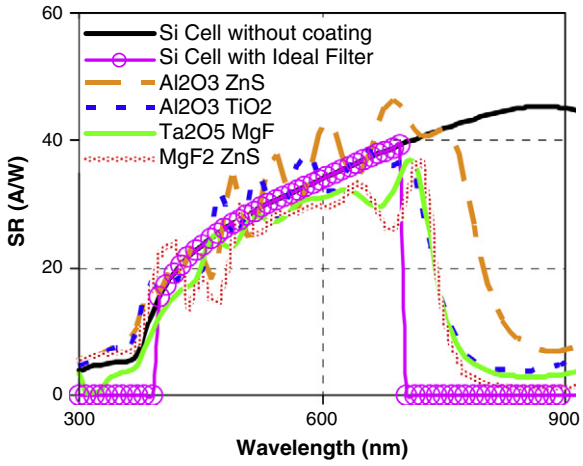

Fig. 7. Simulated spectral response between 300 and 900 nm with dielectric coating of different materials and without coating.

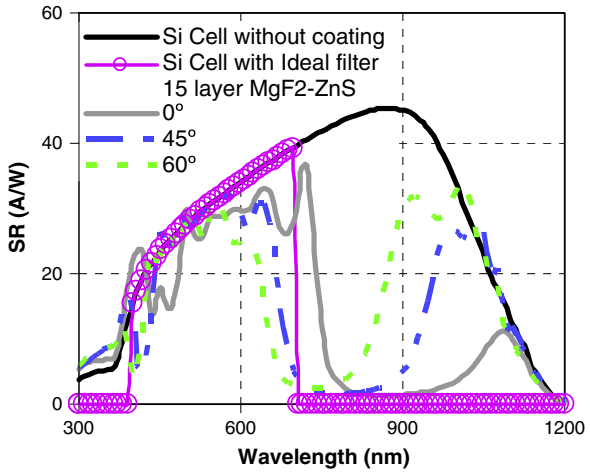

Fig. 8. Variation of the spectral response with the angle of incidence.

Table 7
Calculation of I_{sc} of sensor with 15 layers of MgF_2–ZnS at different angles of incidence.

Angle of incidence	I_{sc} (mA)
0°	1.05
45°	1.09
60°	1.11

I_{sc} was also calculated as in previous cases. For each standard deviation (5 and 10%), several sets of random numbers were taken and the average values for the area under the curve (2.1 and 9.1% respectively) and I_{sc} were calculated (Table 4).

As can be observed, I_{sc} does not show significant differences (~1%) by introducing an uncertainty of 5% in thickness. However, if uncertainty is increased to 10% this difference in I_{sc} rises to 11%.

5. Dielectric coating on sensor

5.1. Calculation of the number of layers

As an alternative to the use of a glass filter the deposition of dielectric layers with high and low index (ZnS and MgF_2 respectively), as shown in Eq. (1), was considered. Sets of 9, 12 and 15 layers deposited on Si were studied using GPL OPTICAL program to simulate spectral reflectance for deposits. These reflectance data were entered into the program PC-1D4 to obtain spectral response for the simulated device. Fig. 6 shows these curves for a bare sensor and 9, 12 and 15 layers, and an ideal filter. The corresponding values of I_{sc} were calculated for the above mentioned configurations and results are shown in Table 5. As in the case of the optical filter, the smallest difference to the ideal filter was found for 15 layer configuration.

5.2. Selection of dielectric materials

Sensor spectral response with dielectric layers was simulated for different combinations of materials to study their behavior, in all cases 15 layers were used. Fig. 7 and Table 6 show the results: in the range of interest the transmittance curve has smaller oscillations for Ta_2O_5–MgF_2 coating. In contrast, the value of the I_{sc} corresponding to a filter made of ZnS–MgF_2 layers is closer to an ideal filter.

5.3. Spectral response as a function of angle of incidence and spectrum

Sensor response for MgF_2–ZnS layers as a function of the angle of incidence was studied in the same way as in the optical filters. The curves are presented in Fig. 8. For angles larger than 45° there is a contribution to I_{sc} from wavelengths longer than 800 nm, however there is no significant change in the value of I_{sc} (Table 7).

To study the influence on I_{sc} due to illumination spectrum, contributions of AM1.5, AM2 and AM3 [20] global (glob) and diffuse (diff) radiation were calculated. I_{sc} was calculated for a bare sensor and with 15 layers of ZnS–MgF_2. The ratio between I_{sc} for AM2 and AM3 spectrum global ($I_{sc\text{-}G}$) and diffuse ($I_{sc\text{-}diff}$) with respect to I_{sc} for the AM1.5 ($I_{scAM1.5}$) spectrum is similar for both the sensor without multilayers and the PAR sensor. Besides it is similar to the ratio of irradiances (H) for these spectra (Table 8).

6. Conclusions

Theoretical simulations of glass filter transmittance and spectral response of multilayer coatings on silicon solar sensor were carried out. The short circuit current (I_{sc}) as a function of the number of layers for a typical sensor with 12 and 15 layer filter was calculated. The difference between I_{sc} calculated for 12 and 15-layer filters and that of the ideal filter was 10% and 6%, respectively. Also, I_{sc} does not show significant differences (~1%) by introducing an uncertainty of 5% in layer thickness. However, if this uncertainty is increased to 10% this difference rises to 11%.

The transmittance curve to obtain a reasonable PAR sensor optical filters and dielectric coatings, indicates that 15 layers is an adequate number of layers to be deposited. Uncertainty in multilayer deposition and standard deviation of up to 10% (equivalent to a thickness of up to 95 Å) were considered. There are ways to correct differences in deposition thicknesses such as through adjustment in successive layers [21], which in this case is considered unnecessary. Finally, layer deposition on Si appears to be more appropriate.

Acknowledgments

The authors acknowledge J.C. Durán, A. Filevich and especially C.J. Bruno for their critical reading of this the manuscript.

References

[1] C.G. Bolzi, C.J. Bruno, J.C. Durán, E.M. Godfrin, M.G. Martínez Bogado, L.M. Merino, J.C. Plá, M.J.L. Tamasi, M. Barrera, Sol. Energy Mater. Sol. Cells 73 (2002) 269.
[2] In: V.S. Kouzmin, G.S. Cheremoukhin, V.I. Fedoseev, M.K. Masten, L.A. Stockum (Eds.), Proceedings — SPIE The International Society for Optical Engineering, Orlando, Florida, E.E.U.U., April 10–17, 2739, 1996, p. 407.
[3] In: J.R. Wertz (Ed.), Spacecraft Attitude Determination and Control, Kluwer Academic Publisher, Dordrecht, Boston, London, 1985.
[4] A.S. Zabiyakin, V.O. Prasolov, A.I. Baklanov, A.V. Eltsov, O.V. Shalnev, Proceedings — SPIE The International Society for Optical Engineering, Prague, Czech Republic, March 10, 3901, 1999, p. 106.
[5] K.J. McCree, Agric. Meteorol. 10 (1972) 443.

Table 8
Calculation of I_{sc} of sensor with and without dielectric layers for different illumination spectra.

Spectrum	H (W/m^2)	H/H (AM1.5)	Without multilayers		With 15 layers of MgF_2–ZnS			
			$I_{sc\text{-}G}$ (mA)	$I_{sc\text{-}diff}$ (mA)	$I_{sc\text{-}G}/I_{scAM15}$	$I_{sc\text{-}G}$ (mA)	$I_{sc\text{-}diff}$ (mA)	$I_{sc\text{-}G}/I_{scAM1.5}$
AM1.5	993	1	2.05	0.24	1	1.17	0.16	1
AM2	858	0.86	1.79	0.22	0.87	1.00	0.14	0.86
AM3	671	0.68	1.41	0.20	0.69	0.76	0.12	0.65

[6] H. Grossi Gallegos, R. Righini, O. Dursi, Av. Energ. Renov. Medio Ambiente 8 (2) (2004) 11.13.
[7] R. Righini, H. Grossi Gallegos, Av. Energ. Renov. Medio Ambiente 9 (2005) 11.01.
[8] C.P. Jacovides, F.S. Timvios, G. Papaioannou, D.N. Asimakopoulos, C.M. Theofilou, Agric. For. Meteorol. 121 (3–4) (2004) 135.
[9] W. Larcher, Physiological Plant Ecology, Ecophysiology and Stress Physiology of Functional Groups, 4th edition Springer-Verlag, Berlin Heidelberg New York, 2003.
[10] R. Frouin, R.T. Pinker, Remote Sens. Environ. 51 (1995) 98.
[11] Q. Wang, J. Tenhunen, M. Schmidt, D. Otieno, O. Kolcun, M. Droesler, Agric. For. Meteorol. 128 (1–2) (2005) 1.
[12] M. Mottus, J. Ross, M. Sulev, Agric. For. Meteorol. 109 (3) (2001) 161.
[13] C.P. Jacovides, F.S. Tymvios, V.D. Assimakopoulos, N.A. Kaltsounides, Agric. For. Meteorol. 143 (3–4) (2007) 277.
[14] R. Righini, H. Grossi Gallegos, C.G. Bolzi, M.G. Martínez Bogado, M.J.L. Tamasi, Av. Energ. Renov. Medio Ambiente 13 (2009) 09.07.
[15] P. Basore, M.J. Gee, M.E. Buck, W.K. Schubert, D.S. Ruby, Sol. Energy Mater. Sol. Cells 34 (1994) 91.
[16] Standard ASTM 1984 N° E, 1984, p. 297-84.
[17] P. Basore, D. Clugston, 26th IEEE Photovoltaic Specialists Conference, Anaheim, California, USA, Sep 28–Oct 5, 1997, p. 207.
[18] M. Born, E. Wolf, Principles of Optics, 6th edición Pergamon Press, New York, 1980.
[19] E. Centurioni, Appl. Opt. 44 (2005) 7532.
[20] C. Gueymard, Sol. Energy 71 (5) (2001) 325.
[21] P. Bousquet, A. Fornier, R. Kowalczyk, E. Pelletier, P. Roche, Thin Solid Films 13 (1972) 285.